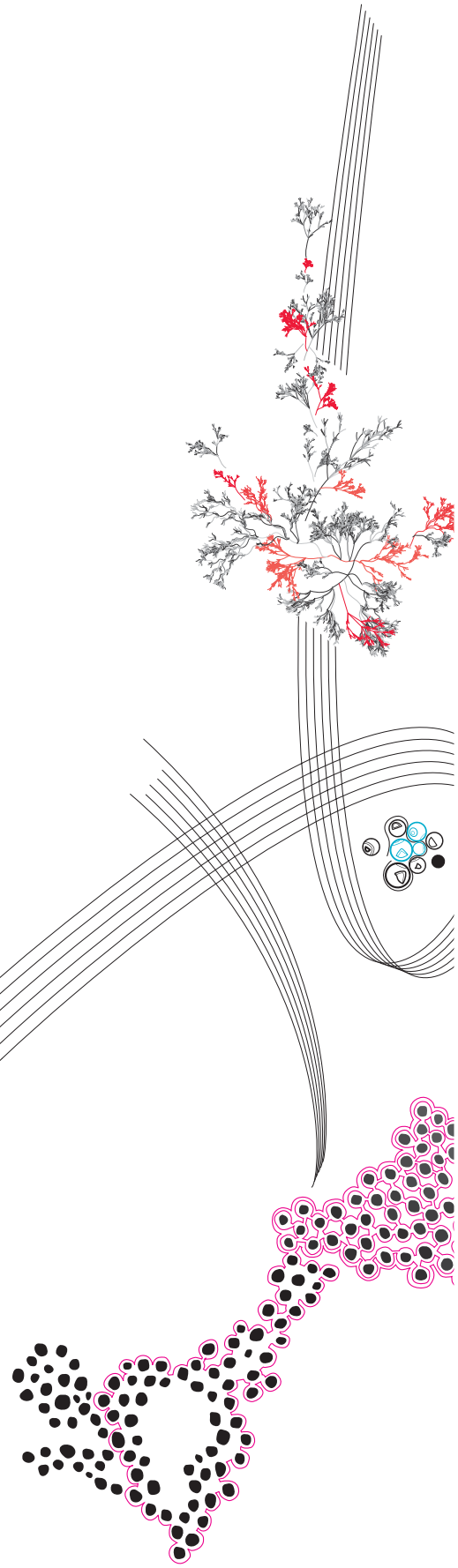

BSc Thesis Applied Mathematics

Reaction-Diffusion patterns modelled by Continuous-State Cellular Automata

Jorn Quattrocchi

Supervisor: dr. M.C. Boldy

June 26, 2020

Department of Applied Mathematics
Faculty of Electrical Engineering,
Mathematics and Computer Science

UNIVERSITY OF TWENTE.

Preface

A special thank you to dr. M. C. Boldy for supervising this research.

Reaction-Diffusion patterns modelled by Cellular Automata

Jorn Quattrocchi*

June 26, 2020

Abstract

This paper contributes to the understanding of reaction-diffusion phenomena, these aesthetically pleasing patterns found in nature and chemistry. No background knowledge is required to investigate a simple model, cellular automata, simulating complex behaviour, reaction-diffusion. Several existing approaches on how to connect cellular automata models and reaction-diffusion systems are discussed. Leading to the introduction of continuous-cell-states eight-cell neighbourhood two-dimensional cellular automata as a model of quasi chemical systems with cell-states resembling continuous flow between a substrate and a reagent. Reaction and diffusion transition rules have been altered to continuous formulas. Simulated cellular automata have been assigned to 12 morphology based classes which have been identified or introduced.
Keywords: reaction-diffusion, cellular automata, continuous state, morphology classes

1 Introduction

Reaction-diffusion models simulate chemical like processes, often described by a set of partial derivatives. The model can simulate the propagation of interesting and aesthetically pleasing periodic patterns in nature and chemistry. The patterns can be a resemblance of a wide range of phenomena, from animal prints to fluid dynamics. Reaction-diffusion typically considers two (hypothetical) chemicals, a substrate and a reagent, but can be extended to more than two different types of chemicals. The reaction and diffusion of the model is often described by partial derivatives. Simulating reaction-diffusion models with a set of partial derivatives requires high computational capacity and for a non-educated viewer the simulation often loses predictability. The model asks for a discretization of the partial derivatives to make large scale parallel computation possible and gain a more intuitive simulation, while preserving the qualitative aspects of the model.

Cellular automata are discrete models with elegant rules which are easy to understand, but can model complex behavior. A cellular automaton consists of a collection of cells on a grid of a predefined shape. Iterating over discrete time steps, each cell will or will not change its state depending on the state of the cells in its neighbourhood. Given the rules of the automaton and the state of every cell, local changes are always easy to predict. In a two-dimensional binary-state cellular automaton the two possible states of a cell can be considered as a substrate (dead or 0) and a reagent (alive or 1), similar to a reaction-diffusion model. Reaction-diffusion and cellular automata have similar ground rules. Similar possible states and similar change depending on neighbourhood suggests that cellular automata could be a sufficient model for reaction-diffusion patterns. While

*Email: j.l.quattrocchi@student.utwente.nl

local predictability is certain, different approaches in providing the rules for a cellular automaton result in different qualitative results.

The goal of this research is to give a non-educated viewer an intuitive feeling of what is going on when reaction-diffusion patterns are simulated. In this paper the different approaches in making a cellular automaton that models reaction-diffusion patterns will be discussed. Trying to find an environment where someone with a lack of background knowledge should be able to investigate reaction-diffusion patterns with cellular automata. To accomplish this the automata need to have a global predictability over multiple iterations and enough freedom in initializing the automata to cover a wide variety of reaction-diffusion phenomena. After discussing existing different approaches, a continuous-state eight-cell neighborhood two-dimensional cellular automaton that models quasi-chemical systems with a continuous flow between substrate and a reagent is introduced and analyzed.

2 Literature Review

Using lattice gas automata (LGA) has been a popular approach to simulate fluid flows. Being a cellular automaton an LGA contains a grid with cells with a fixed number of possible states. Moving particles are simulated in this grid, a cell can have a present particle with a certain velocity or the cell is empty. Therefore two particles moving in the same direction with identical velocity can never be in the same cell. After each discrete time step the new state of every cell is calculated depending on the velocity of neighboring particles and potential collisions, preserving total mass and total momentum. Not considering collision, every particle will transfer to a cell its velocity is pointed at, maintaining all of its velocity. When collision happens, two particles reaching the same cell, predefined rules determine what will happen. These collision rules are free to adjust depending on the desired qualitative results, but preserving total mass and total momentum is mandatory. A widely used and approved LGA that simulates the Navier-Stokes equations was introduced by Frisch, Hasslacher and Pomeau (FHP). The FHP is an improvement on the model already proposed by Hardy, de Pazzis and Pompeau (HPP) which lacked rotational invariance. This is solved by the FHP by using a triangular instead of a square grid. Due to the limits of computational power, computing the large scale interactions of parallel existing particles in fluid dynamics is often impossible or inefficient. The FHP-model is intended to perform well on simulations which calculates the effects on particles on a parallel and equal basis, which inherits from the use of a cellular automaton. [**1**, **2**]

Lattice gas models are a form of qualitative discrete modeling, using cellular automata as a computational friendly alternative to partial differential equations. This approach is also used in other fields, like the Ising-type models of phase transitions [**3**]. These models are created with respect to a specific phenomenon. Although the developed cellular automaton is often a great macroscopic representation, the rules that determine what happens with the particles each time step are very specific. A more quantitative approach that is applicable on a wider reaction-diffusion range is desired.

A new class of cellular automata was introduced to model reaction-diffusion systems in a quantitatively correct way [**4**]. Multiple sets of partial differential equations can be mapped onto this class to get a cellular automaton. The class provides a generalized way to get a discrete representation of reaction-diffusion systems. To implement the diffusion part of the system the class uses moving averages, which makes the calculation of the neighbourhood of every cell very efficient. The averaging itself has the effect of diffusion. The reaction part of the model is implemented by discretizing the rate law of the system,

making it possible to use a lookup table. Discretization can result in incorrect steady states or oscillations. The class solves this by using probabilistic rules to determine whether the cell takes on a new value, making sure the average result still corresponds to the reaction-diffusion equations. The wide applicability of the class is as desired, but switching to different systems requires time and knowledge. Therefore this approach is not sufficient.

The approaches discussed so far are constructed from a reaction-diffusion perspective. The goal of the approaches is to make a cellular automaton that provides qualitative calculations of a certain reaction-diffusion phenomenon. Also the discussed proposed class, which is rather quantitative than qualitative, maps reaction-diffusion systems onto cellular automata. The model might be more intuitive if the approach starts with a systematic investigation of all cellular automata rules within a certain domain. Providing identified classes within its domain containing automata that behave like chemical processes, mapping reaction-diffusion phenomena onto the cellular automata.

Binary-cell-states eight-cell neighbourhood two-dimensional cellular automata have been investigated as a model of a quasi-chemical system with a substrate and a reagent [**5**]. The two-dimensional grid is defined by its coordinates $x, y \,\epsilon\, \mathbb{Z}$, every cell $\mathbf{c}$ has a unique vector representation: $\mathbf{c} = \begin{pmatrix} x \\ y \end{pmatrix}$. The neighbourhood N_8 of $\mathbf{c}$ is defined as a set of 8 cells closest to cell $\mathbf{c}$:

$$N_8(\mathbf{c}) = \{\mathbf{c} + \mathbf{d} \mid \mathbf{d} \,\epsilon\, \{\begin{pmatrix} 0 \\ 1 \end{pmatrix}, \begin{pmatrix} 1 \\ 0 \end{pmatrix}, \begin{pmatrix} 0 \\ -1 \end{pmatrix}, \begin{pmatrix} -1 \\ 0 \end{pmatrix}, \begin{pmatrix} 1 \\ 1 \end{pmatrix}, \begin{pmatrix} -1 \\ 1 \end{pmatrix}, \begin{pmatrix} 1 \\ -1 \end{pmatrix}, \begin{pmatrix} -1 \\ -1 \end{pmatrix}\}\}$$

The cell-state of cell $\mathbf{c}$ at time step t, $s^t(\mathbf{c})$, can only be in one of two possible states: $s^t(\mathbf{c}) \,\epsilon\, \{0, 1\}$ for every cell $\mathbf{c}$. Cell-state 0 can be interpreted as a dead cell or as the substrate and cell-state 1 as an alive cell or as the reagent. For every cell $\mathbf{c}$ in the grid, the state $s^{t+1}(\mathbf{c})$ depends on $s^t(\mathbf{c})$ and the states of the cells in the neighbourhood $N_8(\mathbf{c})$ at time step t. The states of the neighbourhood of $\mathbf{c}$ at time step t are summed together to get:

$$\sigma^t(\mathbf{c}) = \sum_{\mathbf{n} \,\epsilon\, N_8(\mathbf{c})} s^t(\mathbf{n})$$

The neighbourhood of every cell $\mathbf{c}$ contains 8 other cells, so $0 \leq \sigma^t(\mathbf{c}) \leq 8$ always holds. Let $\delta_1, \delta_2, \theta_1, \theta_2$ be integers holding: $0 \leq \delta_1 \leq \delta_2 \leq 8$ and $0 \leq \theta_1 \leq \theta_2 \leq 8$. Interval $[\delta_1, \delta_2]$ is defined as the reaction interval and interval $[\theta_1, \theta_2]$ as the diffusion interval. If $s^t(\mathbf{c}) = 1$ at time step t, then at time step $t + 1$ cell $\mathbf{c}$ stays in state 1 if and only if $\sigma^t(\mathbf{c})$ lies in reaction interval $[\delta_1, \delta_2]$. If $s^t(\mathbf{c}) = 0$ at time step t, then at time step $t + 1$ cell $\mathbf{c}$ changes its state into 1 if and only if $\sigma^t(\mathbf{c})$ lies in diffusion interval $[\theta_1, \theta_2]$. As a result, at time step t every cell $\mathbf{c}$ updates its state $s^t(\mathbf{c})$ by the rule:

$$s^{t+1}(\mathbf{c}) = \begin{cases} 1 & \text{if } (s^t(\mathbf{c}) = 0 \text{ and } \sigma^t(\mathbf{c}) \,\epsilon\, [\theta_1, \theta_2]) \text{ or } (s^t(\mathbf{c}) = 1 \text{ and } \sigma^t(\mathbf{c}) \,\epsilon\, [\delta_1, \delta_2]) \\ 0 & \text{otherwise} \end{cases}$$

The selection of interval boundaries $\delta_1, \delta_2, \theta_1, \theta_2$ decides the cell-state transition rules and thus the propagation of the automaton. The automaton is unique for every possible set of interval boundaries and from now on denoted by: $R(\delta_1, \delta_2, \theta_1, \theta_2)$, Conway's Game of Life is one of the configurations: $R(2, 3, 3, 3)$.

The patterns produced by cellular automata for all 1296 possible rules, $1 \leq \delta_1 \leq \delta_2 \leq 8$ and $1 \leq \theta_1 \leq \theta_2 \leq 8$, were analyzed, initializing the automaton by assigning every cell state 1 with probability 0.3. Ten morphology-based classes of rules were discovered and identified:

Table 1: Discovered classes in binary-cell-states eight-cell neighbourhood two-dimensional cellular automata

Class	**Patterns (after 100 iterations)**	**Examples**
E-class	(Almost) uniform 0-state	R(3,3,c,d), $5 \leq c \leq d \leq 8$ R(4,4,c,d), $4 \leq c \leq d \leq 8$ R(4,5,c,d), $4 \leq c \leq d \leq 8$
S-class	Few small clusters of 1-states	R(1,1,c,d), $3 \leq c \leq d \leq 8$ R(2,2,c,d), $4 \leq c \leq d \leq 8$
D-class	(Almost) uniform 1-state	R(a,8,c,8), $a = 2, 3$ and $1 \leq c \leq 4$ $a = 4, 5$ and $1 \leq c \leq 3$
L-class	Labyrinth structures with walls 1 cell thick (L_1) and walls more than 1 cell thick (L_2)	L_1: R(1,3,1,2), R(1,3,2,2) L_2: R(1,6,1,6), R(4,6,1,7)
M-class	Irregular branching structures	R(1,3,1,5), R(1,4,2,5), R(2,2,1,3), R(2,8,5,8)
P-class	0-state domains containing scattered 1-states and 1-state domains containing scattered 0-states	R(2,3,1,8), R(2,4,1,8)
O-class	Irregular distribution of spots, (dis)connected small clusters of 1-states	R(3,5,1,1), R(3,8,1,1)
G-class	Supporting mobile localizations, or gliders	R(2,b,2,2), $2 \leq b \leq 8$
V-class	Vonoroi-diagram	R(1,6,3,4), R(1,8,3,4), R(4,8,3,4)
C-class	Convex sets of 1-states	R(4,8,4,7), R(4,8,4,8)

The binary-cell-states eight-cell neighbourhood two-dimensional cellular automata have a lot of freedom in initializing the automaton and covers at least ten different classes with propagation of reaction-diffusion like patterns. This approach suits the goal of this research.

3 Continuous-state Cellular Automata

For this research a new domain of cellular automata is introduced and analyzed. By allowing the cell-state to have any value inside the continuous interval [0, 1] the model supports continuous flow between substrate and reagent. Allowing a cell to represent different particles instead of a single one. To implement the continuous-cell-states, while maintaining the simplicity of a cellular automaton, minor adjustments have been made to the binary-cell-states eight-cell neighbourhood two-dimensional cellular automata discussed above. Using the same terminology, the continuous-cell-states eight-cell neighbourhood two-dimensional cellular automata consists of cells with a unique vector representation: $\mathbf{c} = \begin{pmatrix} x \\ y \end{pmatrix}$ with $x, y \in \mathbb{Z}$. And an eight-cell neighbourhood $N_8(\mathbf{c})$ is defined as follows:

$$N_8(\mathbf{c}) = \{\mathbf{c} + \mathbf{d} \mid \mathbf{d} \in \{\begin{pmatrix} 0 \\ 1 \end{pmatrix}, \begin{pmatrix} 1 \\ 0 \end{pmatrix}, \begin{pmatrix} 0 \\ -1 \end{pmatrix}, \begin{pmatrix} -1 \\ 0 \end{pmatrix}, \begin{pmatrix} 1 \\ 1 \end{pmatrix}, \begin{pmatrix} -1 \\ 1 \end{pmatrix}, \begin{pmatrix} 1 \\ -1 \end{pmatrix}, \begin{pmatrix} -1 \\ -1 \end{pmatrix}\}\}$$

Cell-state, $r^t(\mathbf{c})$, of a cell $\mathbf{c}$ at time step t can take on any real value inside the interval [0, 1]: $r^t(\mathbf{c}) \in [0, 1]$. Considering the automata to be a representation of quasi-chemical processes with a substrate and a reagent, the continuous-cell-states allow both a substrate

and a reagent to be present in cell $\mathbf{c}$. The value of $r^t(\mathbf{c})$ can be interpreted as the fraction of reagent particles in cell $\mathbf{c}$. The remaining fraction of the cell, $1-r^t(\mathbf{c})$, can be interpreted as the substrate. For every cell $\mathbf{c}$ in the grid, the state $r^{t+1}(\mathbf{c})$ depends on $r^t(\mathbf{c})$ and the states of the cells in the neighbourhood $N_8(\mathbf{c})$ at time step t. The states of the neighbourhood of $\mathbf{c}$ at time step t are summed together, similarly to the binary-state case, to get:

$$\rho^t(\mathbf{c}) = \sum_{\mathbf{n}\ \epsilon\ N_8(\mathbf{c})} r^t(\mathbf{n})$$

The neighbourhood of every cell $\mathbf{c}$ contains 8 other cells with continuous states, so $\rho^t(\mathbf{c})\ \epsilon\ [0, 8]$ always holds and $\rho^t(\mathbf{c})$ can take on any real value in the interval [0, 8]. Analogously, let $\delta_1, \delta_2, \theta_1, \theta_2$ be integers holding: $0 \leq \delta_1 \leq \delta_2 \leq 8$ and $0 \leq \theta_1 \leq \theta_2 \leq 8$, defining reaction interval: $[\delta_1, \delta_2]$ and diffusion interval: $[\theta_1, \theta_2]$. Because $r^t(\mathbf{c})$ can take on any real value in the interval [0, 1], instead of 0 and 1, the propagation rules of the automaton need to be adjusted. Handling the reaction part of the propagation with reaction rule: $R^t_{\delta_1,\delta_2}(\mathbf{c})$ and handling the diffusion part of the propagation with diffusion rule: $D^t_{\theta_1,\theta_2}(\mathbf{c})$. In addition to the necessary adjustments, the continuous states also opened up the possibility to change the discrete propagation rules of a cellular automaton to continuous propagation rules. Taking the reaction rule as an example, gradually increasing the reaction rate from $\delta_1 - \frac{1}{2}$ to $\delta_1 + \frac{1}{2}$ results in a continuous function around the left edge δ_1 of the reaction interval. Similarly gradually decreasing around the right edge δ_2 results in a completely continuous function for the reaction rule, see *Fig. 1.* Applying the same strategy to the diffusion rule leads to the following definitions. First considering the special cases $\delta_1 = \delta_2$ and $\theta_1 = \theta_2$:

$$R^t_{\delta_1,\delta_2}(\mathbf{c}) = \begin{cases} 1 & \text{if } \rho^t(\mathbf{c}) = \delta_1 = \delta_2 \\ 0 & \text{otherwise} \end{cases}$$

$$D^t_{\theta_1,\theta_2}(\mathbf{c}) = \begin{cases} 1 & \text{if } \rho^t(\mathbf{c}) = \theta_1 = \theta_2 \\ 0 & \text{otherwise} \end{cases}$$

Followed by the general definitions:

$$R^t_{\delta_1,\delta_2}(\mathbf{c}) = \begin{cases} 1 & \text{if } \delta_1 + \frac{1}{2} \leq \rho^t(\mathbf{c}) \leq \delta_2 - \frac{1}{2} \\ \rho^t(\mathbf{c}) - \delta_1 + \frac{1}{2} & \text{if } \delta_1 - \frac{1}{2} < \rho^t(\mathbf{c}) < \delta_1 + \frac{1}{2} \\ \delta_2 - \rho^t(\mathbf{c}) + \frac{1}{2} & \text{if } \delta_2 - \frac{1}{2} < \rho^t(\mathbf{c}) < \delta_2 + \frac{1}{2} \\ 0 & \text{otherwise} \end{cases}$$

$$D^t_{\theta_1,\theta_2}(\mathbf{c}) = \begin{cases} 1 & \text{if } \theta_1 + \frac{1}{2} \leq \rho^t(\mathbf{c}) \leq \theta_2 - \frac{1}{2} \\ \rho^t(\mathbf{c}) - \theta_1 + \frac{1}{2} & \text{if } \theta_1 - \frac{1}{2} < \rho^t(\mathbf{c}) < \theta_1 + \frac{1}{2} \\ \theta_2 - \rho^t(\mathbf{c}) + \frac{1}{2} & \text{if } \theta_2 - \frac{1}{2} < \rho^t(\mathbf{c}) < \theta_2 + \frac{1}{2} \\ 0 & \text{otherwise} \end{cases}$$

Because $\delta_1, \delta_2, \theta_1, \theta_2$ are integers and the special cases $\delta_1 = \delta_2$ and $\theta_1 = \theta_2$ have their own definition, reaction rule: $R^t_{\delta_1,\delta_2}(\mathbf{c})$ and diffusion rule: $D^t_{\theta_1,\theta_2}(\mathbf{c})$ are now defined sufficiently. If $0 < \rho^t(\mathbf{c}) < 1$, then the reaction rule, $R^t_{\delta_1,\delta_2}(\mathbf{c})$, and the diffusion rule, $D^t_{\theta_1,\theta_2}(\mathbf{c})$, both need to be applied to cell $\mathbf{c}$. Clearly, each rule should be weighted proportionately to the state $\rho^t(\mathbf{c})$ of cell $\mathbf{c}$, therefor every cell $\mathbf{c}$ updates its state $\rho^t(\mathbf{c})$ by the rule:

$$\rho^{t+1}(\mathbf{c}) = \rho^t(\mathbf{c}) R^t_{\delta_1,\delta_2}(\mathbf{c}) + (1 - \rho^t(\mathbf{c})) D^t_{\theta_1,\theta_2}(\mathbf{c})$$

In this way the integrity of a reaction-diffusion system with a substrate and a reagent stays intact. A cell with a low state $\rho^t(\mathbf{c})$ has little reagent particles that can react and more space for reagent particles to diffuse into the cell, assigning more weight to the diffusion rule $D^t_{\theta_1,\theta_2}(\mathbf{c})$. Conversely, a cell with a high state $\rho^t(\mathbf{c})$ has many reagent particles that can react and little space for reagent particles to diffuse into the cell, assigning more weight to the reaction rule $R^t_{\delta_1,\delta_2}(\mathbf{c})$. The cellular automata is now defined properly and the selection of interval boundaries $\delta_1, \delta_2, \theta_1, \theta_2$ decides the cell-state transition rules and thus the propagation of the automaton. The automaton is unique for every possible set of interval boundaries and from now on denoted by $R^*(\delta_1, \delta_2, \theta_1, \theta_2)$. As defined the interval boundaries are restricted to: $0 \leq \delta_1 \leq \delta_2 \leq 8$ and $0 \leq \theta_1 \leq \theta_2 \leq 8$. With the new propagation rules it is no longer possible to make the reagent a completely absorbing state, $\rho^t(\mathbf{c}) \leq \rho^{t+1}(\mathbf{c})$ for all $\mathbf{c}$ and any t. Therefor the boundaries of the reaction interval are extended to $-1 \leq \delta_1 \leq \delta_2 \leq 9$, selecting $\delta_1 = -1$ and $\delta_2 = 9$ enables the reagent to be a completely absorbing state.

4 Results

Continuous-cell-states eight-cell neighbourhood two-dimensional cellular automata, as defined above, have been analyzed and classified. All 1296 possible $R^*(\delta_1, \delta_2, \theta_1, \theta_2)$, with $1 \leq \delta_1 \leq \delta_2 \leq 8$ and $1 \leq \theta_1 \leq \theta_2 \leq 8$, have been simulated. As an extension, $\delta_1 = -1, 0$, $1 \leq \delta_2 \leq 9$ with $1 \leq \theta_1 \leq \theta_2 \leq 8$ have been added to enable simulations of an (almost) completely absorbing reagent. Which makes a total of 1944 simulated automata. The state of ten percent of the cells of a 150x150 two-dimensional grid were initially set to 1. After 100 iterations the patterns were analyzed, if the patterns satisfy certain conditions the automata can be added to one of the defined morphology based classes. Classes from the binary-cell-states automata have been used, providing them with new definitions if needed. Some classes have been added for specific continuous-cell-states automata patterns. Assigning an automaton to a certain class can depend, to some extend, on an individual empirical factor, so some automata with unspecific patterns have not been mapped to a class.

The **E-, D-, C-, P-, O-** and **G-**class from binary-states automata can also be mapped onto the continuous-states automata, the definitions are slightly altered to fit the continuous states, see Table 2 for all classes used. The **S-**class from binary-states automata is neglected, since small clusters of 1-states are generally a result of insufficient initial distribution of 1-states. The automata that could have been assigned to the **S-**class are now assigned to the uniform low state **E-**class or not assigned to a class at all.

The **L-** and **M-**class are redefined to reduce the empirical factor. As in the binary-states automata labyrinth-like structures can be found. The **L-**class now only contains labyrinth structures with 1 cell thick walls of high state cells. The area between the walls, low state cells, is usually also 1 cell thick. All other irregular branch-like or labyrinth-like structures are now part of the **M-**class.

The **H-, B-** and **Q-**class have been added for newly discovered behavior. The **H-**class contains automata which look like the automata from the **L-**class, but consist of only horizontal and vertical long 1 cell thick stripes of high state cells altered by 1 cell thick stripes with low state cells. The **B-**class groups automata which propagate to an (almost) uniform distribution of a certain balance between substrate and reagent (cell-states ≈ 0.5), a few small clusters of low or high state cells can be present. The **Q-**class contains automata with a dense distribution of small (1 or 2 cells) disconnected high state cells.

The **E-**class, uniform low states, contains a large portion of the simulated automata,

higher initial distribution of 1-state cells will reduce the number of automata in this class. In that case, automata with similar rules in other classes can give a prediction of the patterns encountered. This class contains, at least, the automata:

$R^*(a,b,c,d)$ with:
$a = -1, 0$; $b = 7, 8, 9$; $5 \leq c \leq d \leq 8$
$a = -1, 0$; $b = 3, 4, 5, 6$; $4 \leq c \leq d \leq 8$
$a = -1, 0$; $b = 1, 2$; $3 \leq c \leq d \leq 8$
$a = 1, 2$; $b = 5, 6, 7, 8$; $4 \leq c \leq d \leq 8$
$a = 1, 2$; $b = 1, 2, 3, 4$; $3 \leq c \leq d \leq 8$
$3 \leq a \leq b \leq 8$; $3 \leq c \leq d \leq 8$
$R^*(a,b,2,3)$ with:
$4 \leq a \leq b \leq 8$

The **D-**class, uniform high states, contains automata with $\delta_1 = -1, 0$ and $\delta_2 = 9$ making the reagent (almost) completely absorbing and enables the state of all cells to stay high. This class contains, at least, the automata:

$R^*(-1,9,c,d)$ with:
$c = 1, 2, 3, 4$; $d = 6, 7, 8$
$R^*(0,9,c,d)$ with:
$c = 1, 2, 3$; $d = 6, 7, 8$

The **M-**class, irregular branching structures, has a lot of freedom in interpretation. A wide variety of branching structures, from thin to thick branches and few to many branches, can be found in the class. This class contains, at least, the automata:

$R^*(a,7,c,d)$ with: $a = -1, 0, 1, 2$; $c = 1, 2, 3$; $d = 7, 8$
$R^*(a,6,c,d)$ with: $a = -1, 0, 1, 2$; $c = 1, 2, 3$; $d = 6, 7, 8$
$R^*(a,5,c,d)$ with: $a = -1, 0, 1$; $c = 1, 2, 3$; $d = 6, 7, 8$
$R^*(a,4,c,d)$ with: $a = -1, 0, 1$; $c = 1, 2, 3$; $d = 5, 6, 7, 8$
$R^*(a,3,c,d)$ with: $a = -1, 0$; $c = 1, 2$; $4 \leq d \leq 8$
$R^*(a,2,1,d)$ with: $a = -1, 0$; $2 \leq d \leq 8$
$R^*(a,2,2,d)$ with: $a = -1, 0$; $d = 4, 5$
$R^*(a,1,1,d)$ with: $a = -1, 0$; $2 \leq d \leq 7$
$R^*(a,1,2,d)$ with: $a = -1, 0$; $d = 4, 5$
$R^*(3,7,c,d)$ with: $c = 1, 2$; $d = 7, 8$
$R^*(3,6,c,d)$ with: $c = 1, 2$; $d = 6, 7, 8$
$R^*(4,8,c,8)$ with: $c = 1, 2$
$R^*(4,b,c,d)$ with: $b = 5, 6, 7$; $c = 1, 2$; $d = 7, 8$
$R^*(a,b,1,3)$ with: $6 \leq a \leq b \leq 8$

The **L-**class, labyrinth structures with 1 cell thick walls, is very specified. Nevertheless, the automata that satisfy the definition of the **L-**class are easily recognized. This class contains at least, the automata:

$R^*(a,7,c,d)$ with:
$a = -1, 0, 1$; $c = 2$; $d = 2, 3, 4, 5$
$a = -1, 0, 1$; $c = 3$; $d = 3, 4, 5$

$R^*(a, 6, c, d)$ with:
$a = -1, 0, 1$; $c = 2$; $d = 3, 4$
$a = -1, 0, 1$; $c = 3$; $d = 3$
$R^*(a, 5, c, d)$ with:
$a = -1, 0, 1$; $c = 1$; $d = 3, 4$
$a = -1, 0, 1$; $c = 2$; $d = 2, 3, 4$
$a = -1, 0, 1$; $c = 3$; $d = 3, 4$
$R^*(a, 4, c, d)$ with:
$a = -1, 0$; $c = 1$; $d = 1, 2, 3$
$a = -1, 0$; $c = 2$; $d = 2, 3$
$a = -1, 0$; $c = 3$; $d = 3, 4$
$R^*(a, 3, c, d)$ with:
$a = -1, 0$; $c = 1$; $d = 1$
$a = -1, 0$; $c = 2$; $d = 2$
$R^*(2, 7, 3, d)$ with:
$d = 3, 4, 5$
$R^*(3, 3, 2, d)$ and $R^*(4, 4, 2, d)$ with:
$d = 6, 7, 8$
$R^*(5, b, c, d)$ with:
$b = 5, 6, 7, 8$; $c = 1$; $d = 7, 8$
$b = 5, 6, 7, 8$; $c = 2$; $d = 6, 7, 8$
$R^*(a, b, c, d)$ with:
$6 \leq a \leq b \leq 8$; $c = 2$; $d = 6, 7, 8$

The **C-**class, convex medium to high state cell clusters, is quite specific. Therefor it contains only a few automata. Convex clusters are formed, because the reaction rule $[\delta_1, \delta_2]$ does not allow branches to form. This class contains, at least, the automata:

$R^*(3, b, 2, 3)$ with: $4 \leq b \leq 8$

The **P-**class, low state domains with scattered high state clusters and high state domains with scattered low state clusters, contains some very obvious cases like $R^*(1, 2, 1, 8)$, see Fig. 7(a). But with a wider reaction interval and a more narrow diffusion interval, the cases become more blurry to a point where the automaton comes really close to some automata in the **M-**class, like $R^*(2, 4, 1, 7)$, see Fig. 7(c). This class contains, at least, the automata:

$R^*(1, 3, c, d)$ with:
$c = 1$; $d = 8$
$c = 2$; $d = 7, 8$
$R^*(a, 5, 1, d)$ with:
$a = 2, 3$; $d = 7, 8$
$R^*(a, 4, c, d)$ with:
$a = 2, 3$; $c = 1$; $d = 8$
$a = 2, 3$; $c = 2$; $d = 7, 8$
$R^*(2, 3, c, d)$ with:
$c = 1$; $d = 6, 7, 8$
$c = 2$; $d = 8$
$R^*(3, 3, 1, d)$ with:

$d = 7, 8$
$R^*(4, b, 1, 3)$ with:
$b = 5, 6, 7$
$R^*(5, b, 1, d)$ with:
$b = 6, 7, 8$; $d = 3, 4$
$R^*(a, b, 1, d)$ with:
$6 \leq a \leq b \leq 8$; $d = 4, 5$

The **O-**class, (dis)connected clusters (4 cells) of high states, has automata with diffusion interval: $[\theta_1, \theta_2] = [1, 1]$ and a lower boundary of reaction interval: $\delta_1 = 2$. This means that low state cells, with cumulative neighbouring cell states of 1, are trying to change into high state cells. But the next iteration the newly formed high state cells are brought back to low state cells, since their cumulative neighbouring cell states will not exceed the lower boundary of the reaction interval. This class contains, at least, the automata:

$R^*(2, b, 1, 1)$ with: $b = 5, 6, 7, 8$

The **V-**class contains automata which show Vonoroi-diagrams. Because the reaction interval is wide, the reagent is (almost) completely absorbing. With a random initial distribution, some places in the grid have more high states than other places. The clusters of cells that satisfy the narrow diffusion interval of the automata will start to spread. Growing domains of high state cells meet each other eventually, but will not merge because the narrow line of low state cells between both domains will then exceed the narrow diffusion interval. As a result, the automata propagate to Vonoroi-diagrams, each cell in a high state domain is closest to the initial cluster that formed its domain. This class contains, at least, the automata:

$R^*(-1, 9, c, d)$ with:
$c = 2$; $d = 4, 5$
$c = 3$; $d = 3, 4, 5$
$R^*(0, 9, c, d)$ with:
$c = 2$; $d = 3, 4, 5$
$c = 3$; $d = 4, 5$
$R^*(a, 8, 3, d)$ with:
$a = -1, 0, 1$; $d = 4, 5$
$R^*(2, 8, c, d)$ with:
$c = 2$; $d = 3, 4, 5$
$c = 3$; $d = 4, 5$
$R^*(2, 7, 2, 3)$

The **H-**class, 1 cell thick stripes of high and low states, consists of automata which diffusion interval $[\theta_1, \theta_2]$ is only 1 or 2 more wide than cases of the **L-**class. The automata from both classes are very similar, but the stripes are easily identified making it possible to have separate classes. This class contains, at least, the automata:

$R^*(a, 6, c, d)$ with:
$a = -1, 0, 1$; $c = 1, 2, 3$; $d = 5$
$a = -1, 0, 1$; $c = 3$; $d = 4$
$a = 2$; $c = 3$; $d = 4, 5$

$R^*(a, 5, 3, 5)$ with:
$a = -1, 0, 1$
$R^*(a, 4, 2, 4)$ with:
$a = -1, 0, 1$
$R^*(a, 3, c, d)$ with:
$a = -1, 0, 1$; $c = 1$; $d = 2$
$a = -1, 0, 1$; $c = 2$; $d = 3$

The **B-**class, uniform balance between substrate and reagent (most cell states ≈ 0.5), contains automata which are able to propagate to an (almost) uniform medium state. The sum of the states of neighbouring cells will become steady when the value of the sum is around 4, because $\delta_1 = 4$ and $\theta_2 = 4$. When (almost) every cell has a state equal to approximately 0.5, the sum of the states of the neighbouring cells will be approximately 4 for every cell and thus steady. This class contains, at least, the automata:

$R^*(4, b, 2, 4)$ with: $b = 5, 6, 7, 8$

The **Q-**class, dense distribution of small (1 or 2 cells) disconnected high state dots, only contains 3 automata. The behavior of the class can only be encountered at specific small and low reaction and diffusion intervals. This class contains, at least, the automata:

$R^*(-1, b, c, d)$ with:
$b = 1$; $c = 1$; $d = 1$
$b = 2$; $c = 1$; $d = 1$
$b = 2$; $c = 2$; $d = 2$

The **G-**class, supporting mobile localizations (gliders), is different to the other classes. The patterns are not valued after 100 iterations, but the propagation towards generation 100 is analyzed. The automata in this class support mobile localizations, also known as gliders. Gliders are small clusters of cells that periodically return to its initial form only with a small displacement. As a result the gliders will "glide" over the grid. The existence of gliders makes the behavior of the automata very complex, because colliding gliders can result in irregular exploding complex behavior not limited to the position of the initial clusters. The automata $R^*(1, 2, 2, 2)$ also supports gliders. Usually this leads to complex behaviour, but the narrow low reaction interval (1, 2) will lead to the vanishing of most high state cells. After a few generations, only glider formation will be present in the simulation, see Fig. 13. This class contains, at least, the automata:

$R^*(a, b, 2, 2)$ with:
$a = 0$; $b = 1$
$a = 1$; $b = 2, 3, 4$
$a = 2$; $b = 3, 4, 5$
$3 \leq a \leq b \leq 8$

Table 2: Discovered classes in continuous-cell-states eight-cell neighbourhood two-dimensional cellular automata

Class	**Patterns (after 100 iterations)**	**Examples**
E-class	(Almost) uniform low-state cells	See Fig. 2
D-class	(Almost) uniform high-state cells	See Fig. 3
M-class	Irregular branching structures of high-state cells	See Fig. 4
L-class	Labyrinth structures with walls of high state cells, 1 cell thick.	See Fig. 5
C-class	Uniform low-state cells with stable convex clusters of medium to high state cells	See Fig. 6
P-class	Low state domains containing scattered high states and high state domains containing scattered low states	See Fig. 7
O-class	Irregular distribution of spots, (dis)connected small clusters (4-cells) of high states	See Fig. 8
V-class	Vonoroi-diagram, every domain of high states is separated by a fine line of low states	See Fig. 9
H-class	Almost completely covered by long lines of 1 cell thick high states altered by 1 cell thick low states	See Fig. 10
B-class	(Almost) uniform medium-state (≈ 0.5) cells	See Fig. 11
Q-class	Dense distribution of small (1 or 2 cells) disconnected high state dots	See Fig. 12
G-class	Supporting mobile localizations, or gliders	See Fig. 13

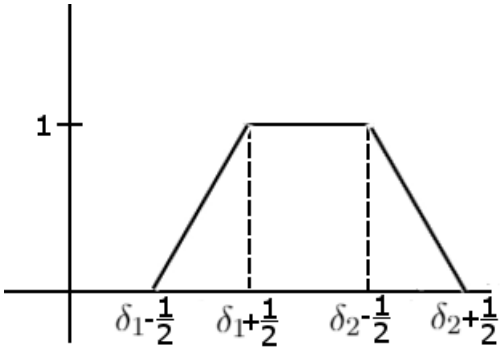

Figure 1: Continuous reaction rule: $R^t_{\delta_1,\delta_2}(\mathbf{c})$

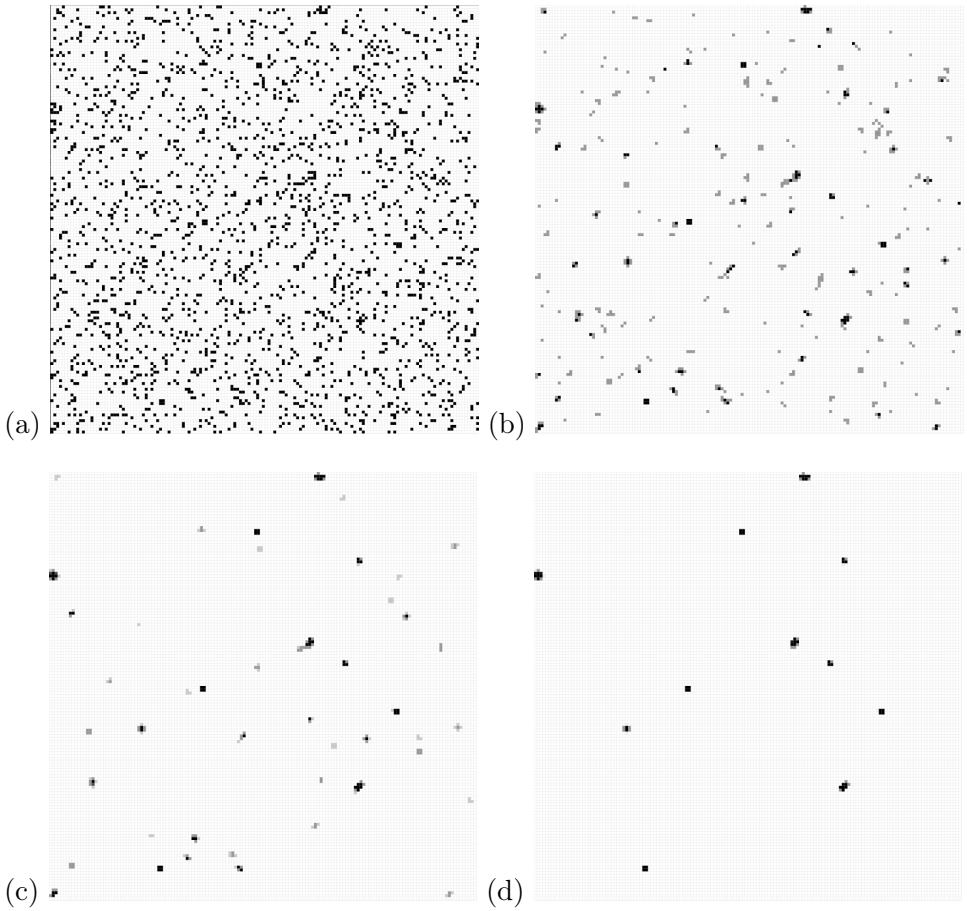

Figure 2: propagation of $R^*(2,8,4,8)$ member of the **E-**class: (a) Generation 0, (b) Generation 1, (c) Generation 2, (d) Generation 10. Initial cells set to state 1 with a chance of 0.1 in a grid of 150x150 cells.

(a) 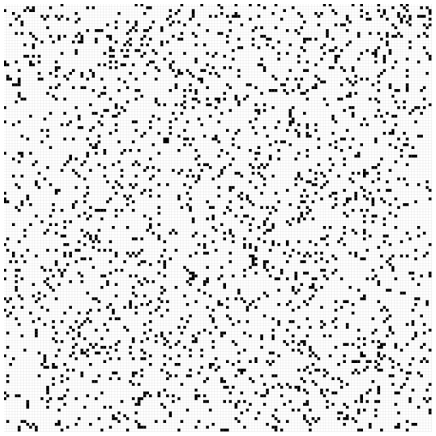 (b) 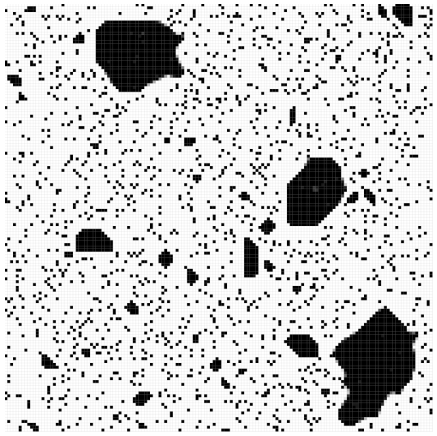

(c) 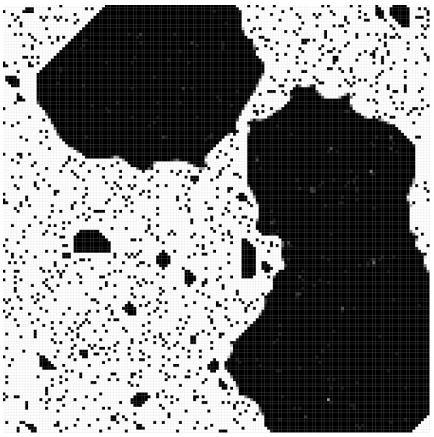

Figure 3: propagation of $R^*(-1, 9, 4, 6)$ member of the **D-**class: (a) Generation 0, (b) Generation 100, (c) Generation 300. Initial cells set to state 1 with a chance of 0.1 in a grid of 150x150 cells.

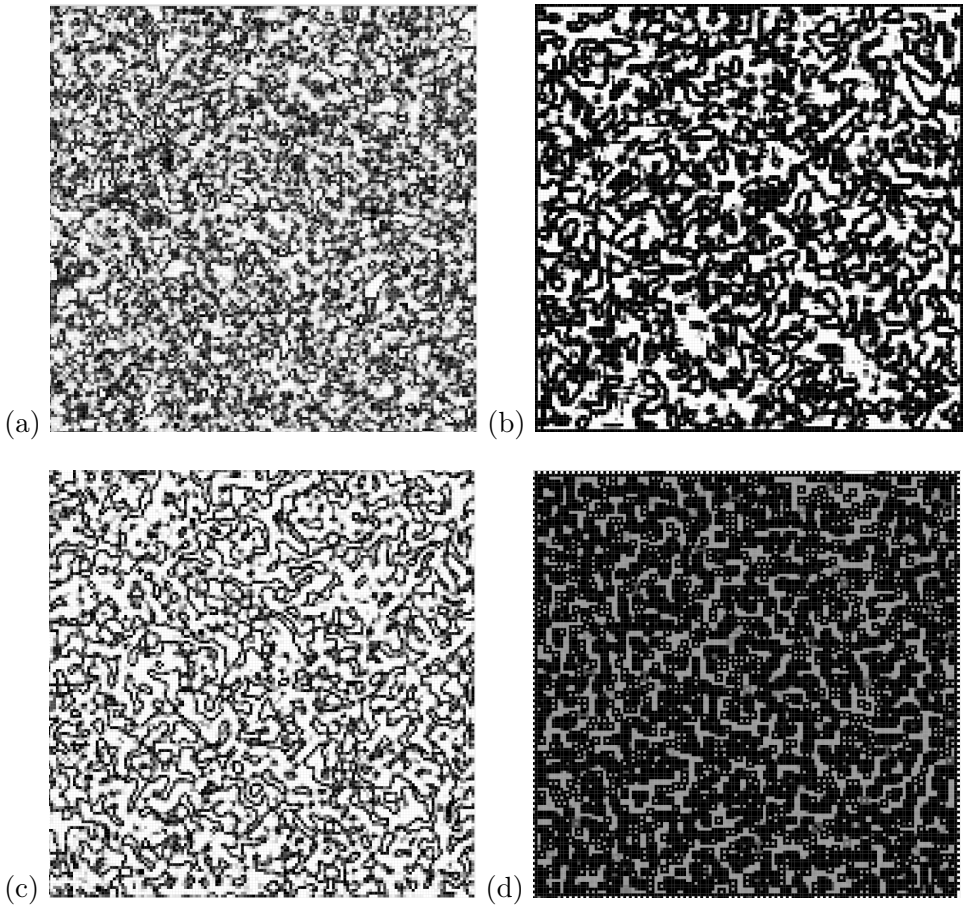

Figure 4: examples of automata in the **M-**class: (a) $R^*(-1,3,2,6)$, (b) $R^*(-1,6,1,6)$, (c) $R^*(1,2,1,4)$, (d) $R^*(4,8,1,8)$. Initial cells set to state 1 with a chance of 0.1 in a grid of 150x150 cells, images are of generation 100.

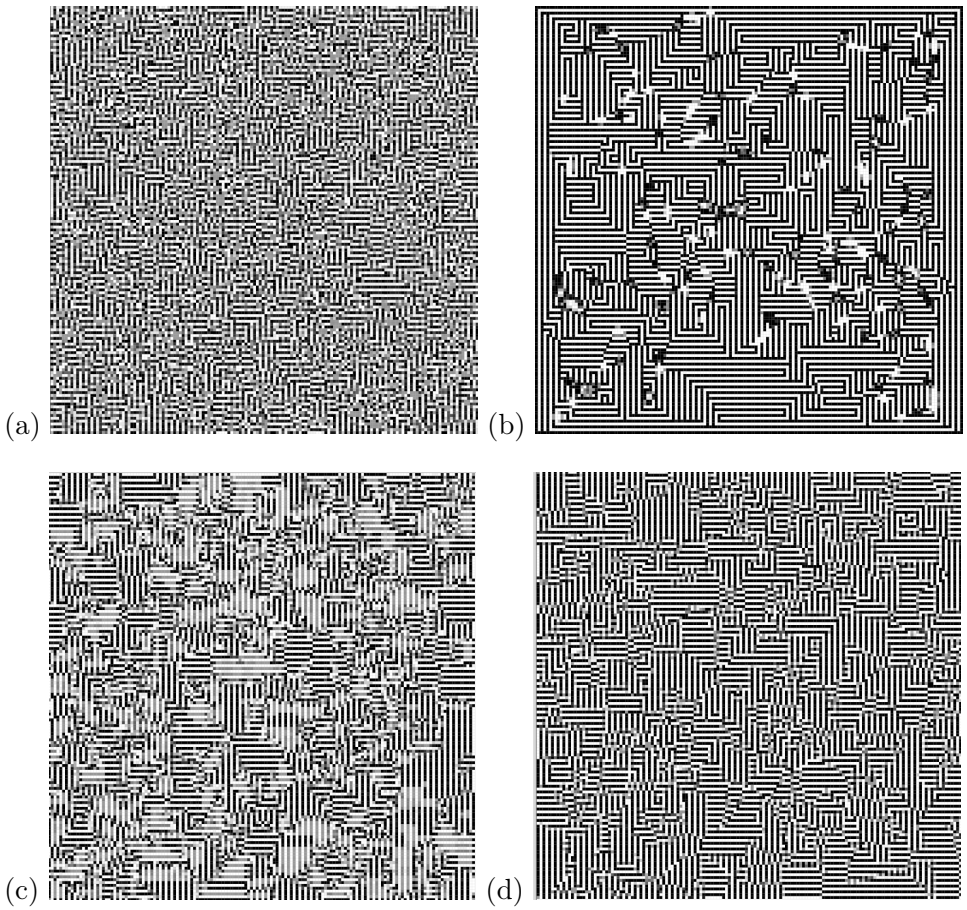

Figure 5: examples of automata in the **L**-class: (a) $R^*(-1,1,2,7)$, (b) $R^*(-1,5,1,4)$, (c) $R^*(4,4,2,6)$, (d) $R^*(6,7,2,8)$. Initial cells set to state 1 with a chance of 0.1 in a grid of 150x150 cells, images are of generation 100.

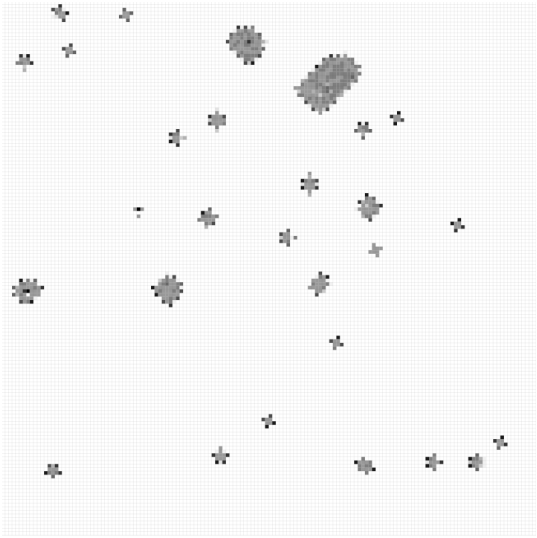

Figure 6: example of the **C-**class: $R^*(3, 8, 2, 3)$. Initial cells set to state 1 with a chance of 0.1 in a grid of 150x150 cells, image is of generation 100.

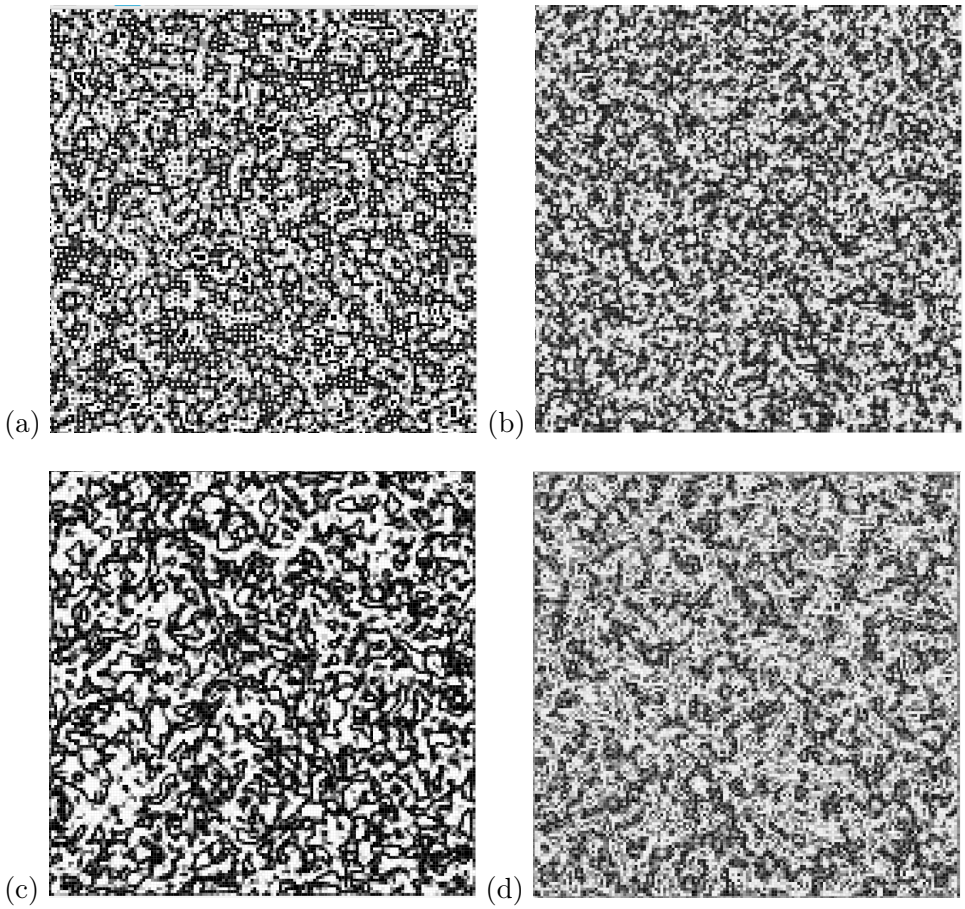

Figure 7: examples of automata in the **P-**class: (a) $R^*(1, 2, 1, 8)$, (b) $R^*(1, 3, 2, 8)$, (c) $R^*(2, 4, 1, 7)$, (d) $R^*(5, 6, 1, 4)$. Initial cells set to state 1 with a chance of 0.1 in a grid of 150x150 cells, images are of generation 100.

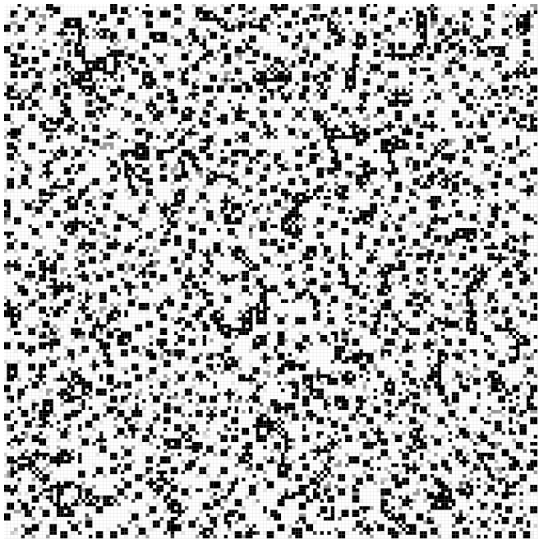

Figure 8: example of the **O-**class: $R^*(2, 8, 1, 1)$. Initial cells set to state 1 with a chance of 0.1 in a grid of 150x150 cells, image is of generation 100.

(a) 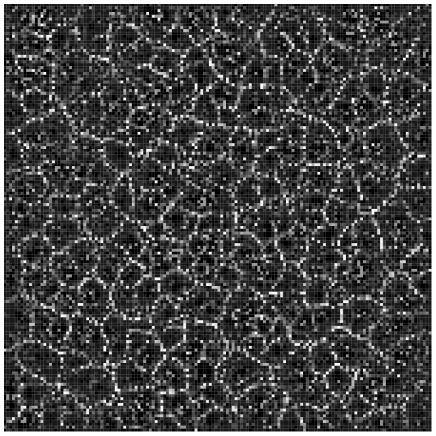 (b) 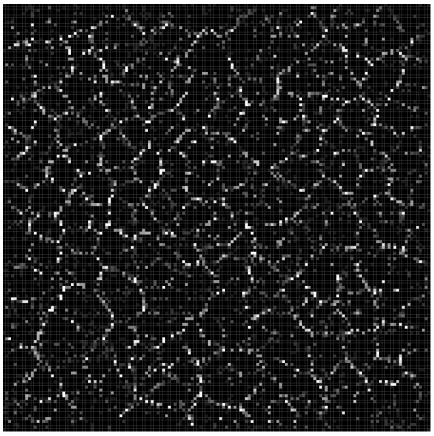

Figure 9: examples of automata in the **V-**class: (a) $R^*(-1, 9, 3, 4)$, (b) $R^*(-1, 9, 3, 5)$. Initial cells set to state 1 with a chance of 0.1 in a grid of 150x150 cells, images are of generation 100.

(a) 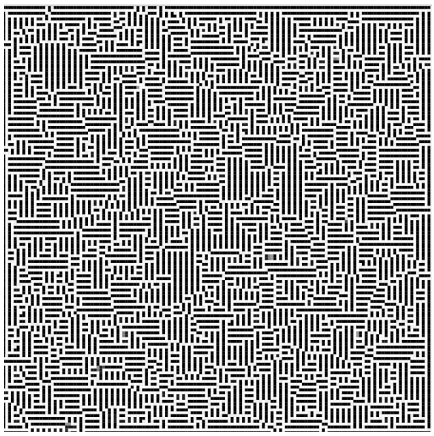 (b) 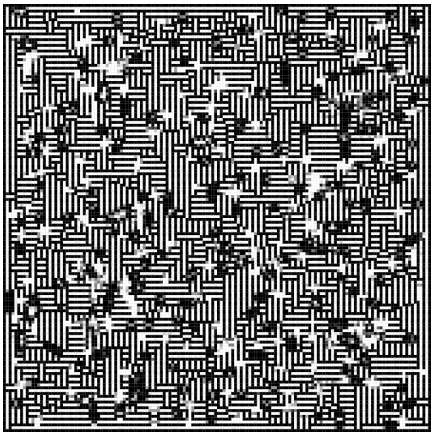

Figure 10: examples of automata in the **H-**class: (a) $R^*(-1,3,1,2)$, (b) $R^*(-1,6,1,5)$. Initial cells set to state 1 with a chance of 0.1 in a grid of 150x150 cells, images are of generation 100.

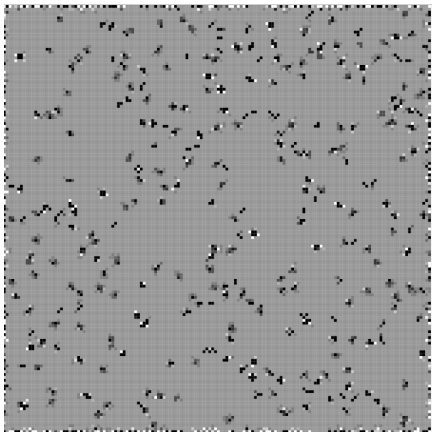

Figure 11: example of the **B-**class: $R^*(4,6,1,4)$. Initial cells set to state 1 with a chance of 0.1 in a grid of 150x150 cells, image is of generation 100.

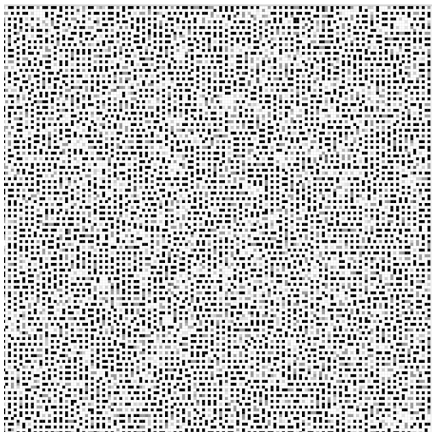

Figure 12: example of the **Q-**class: $R^*(-1,2,1,1)$. Initial cells set to state 1 with a chance of 0.1 in a grid of 150x150 cells, image is of generation 100.

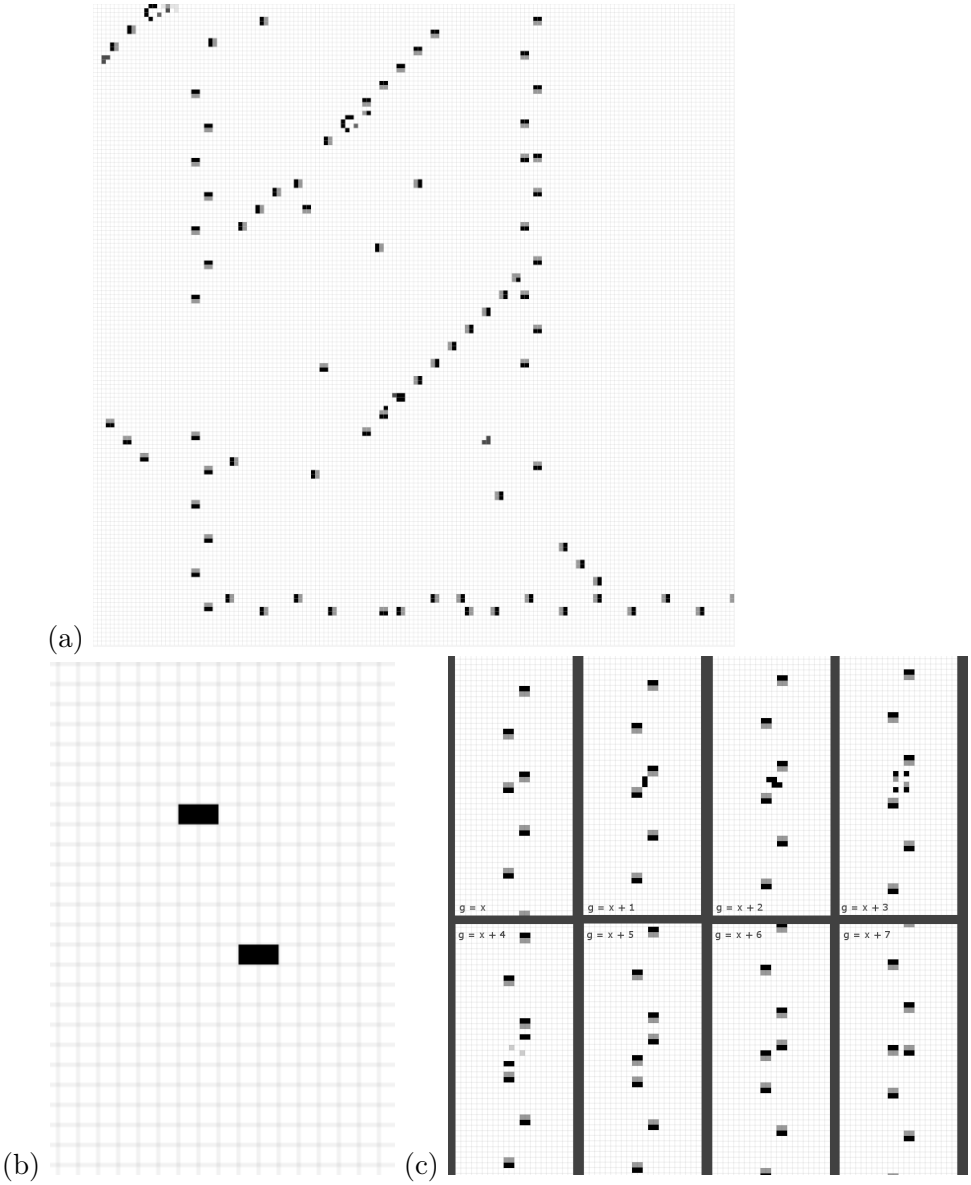

Figure 13: example of automata in the **G-**class: (a) $R^*(1,2,2,2)$, initial cells set to state 1 with a chance of 0.1 in a grid of 150x150 cells, image is of generation 100. (b) $R^*(1,2,2,2)$, initial simple configuration for constant glider formation. (c) $R^*(1,2,2,2)$, 8 iterations of constant glider formation producing 2 gliders (16 iterations is a full cycle,)

5 Conclusion

In this paper different approaches have been discussed to use cellular automata as a model for reaction-diffusion patterns. Systematically analyzing a domain of automata and mapping the patterns simulated by the automata onto reaction-diffusion phenomena turned out to be the most intuitive way to work with complex pattern generation. Two-dimensional cellular automata with continuous cell states and eight-cell neighbourhoods were introduced. A wide range of possible automata have been investigated as a model for reaction-diffusion systems with continuous flow between substrate and reagent. 1944 different automata have been simulated. Some of them have been classified in 12 (re)defined morphology based classes: **E-, D-, M-, L-, C-, P-, O-, V-, H-, B-, Q-** and **G-**class. An environment has been realized where someone with a lack of background knowledge can investigate the possibilities of simulating with a cellular automaton. The provided classes can help in understanding the reaction-diffusion behaviour that will be encountered.

References

[1] A. Gunstensen, D. Rothman, S. Zaleski and G. Zanetti. *Lattice Boltzmann model of immiscible fluids.* Physical Review A, volume 43, 8. 1991.

[2] U. Frisch, B. Hasslacher and Y. Pomeau. *Lattice-gas automata for the Navier-Stokes equation.* Physical review letters, volume 56, 14. 1986.

[3] T. D. Lee and C. N. Yang. *Statistical theory of equations of state and pahse transitions. II. Lattice gas and ising model.* Physical Review, volume 87, 3. 1952.

[4] J. Weimar and J. Boon. *Class of cellular automata for reaction-diffusion systems.* Physical review E, volume 49, 2. 1994.

[5] A. Adamatzky, G. J. Martínez and J. C. S. T. Mora. *Phenomenology of reaction-diffusion binary-state cellular automata.* International Journal of Bifurcation and Chaos, volume 17, 10. 2006.

[6] N. Packard and S. Wolfram. *Two-dimensional cellular automata.* Journal of Statistical physics, volume 38, 5-6. 1985.